

ESTIMATION OF VS30 BASED ON SOIL INVESTIGATION BY USING MICROTREMOR OBSERVATION IN PADANG, INDONESIA

*Rusnardi Rahmat Putra ¹

¹Engineering Faculty, Universitas Negeri Padang, Indonesia

*Corresponding Author, Received: 15 Dec. 2016, Revised: 27 March 2017, Accepted: 24 April 2017

ABSTRACT: Several powerful earthquakes have struck Padang during recent years, one of the largest of which was an M 7.6 event that occurred on September 30, 2009 and caused more than 1000 casualties. Following the event, we performed single observations of microtremors at 110 sites in Padang. The results enabled us to estimate the site-dependent amplification characteristics of earthquake ground-motion. We also conducted a 12-site microtremor array investigation to gain a representative determination of the soil condition of subsurface structures in Padang. From the dispersion curve of array observations, the central business district of Padang corresponds to relatively soft soil condition with V_{S30} less than 400 m/s, the predominant periods due to horizontal vertical ratios (HVSRS) are in the range of 2.0 to 4.0 s.

Keywords: Peak Ground Acceleration, Padang Earthquake, Microtremor Observations.

1. INTRODUCTION

The city of Padang, located on the west coast of Sumatra in western Indonesia, lies close to the Sumatran subduction zone that is formed by the subduction of the Indo-Australian Plate beneath the Eurasian Plate. Relative motion of the plates occurs at a rate of about 50 to 70 mm/year and this is the main source of subduction-related seismicity in the area [1]. Based on our catalog, seven giant earthquakes have occurred in this region since records began: 1779 (Mw 8.4), 1833 (Mw 9.2), 1861 (Mw 8.3), 2004 (Mw 9.2), 2007 (Mw 7.9 and 8.4) and 2009 (Mw 7.6). The hypocenter of the Padang earthquake that occurred on September 30, 2009 was located in the ocean slab of the Indo-Australian Plate at -0.81°S , 99.65°E and at a depth of 80 km. It produced a high degree of shaking and the tremor was felt in the Indonesian capital, Jakarta, about 923 km from the epicenter. The tremors also were felt in neighboring countries such as Malaysia and Singapore. The earthquake caused landslides and collateral debris flows in the hills surrounding Lake Maninjau. A major landslide in Gunung Nan Tigo, Padang Pariaman completely destroyed some villages and forced road closures.

This 1900-km-long active strike-slip fault zone that runs along the backbone of Sumatra poses seismic and fault hazards to a dense population distributed on and around the fault zones. The Sumatran Fault is highly segmented. It consists of 20 major geometrically defined segments and the slip rate along the fault increase to the northwest, from about 5 mm/yr [2]. This fault also has generated large destructive earthquakes, e.g., 1892 (Mw 7.1), 1943 (Mw 7.6) and 2007 (Mw 6.4). These faults are capable of generating strong ground motion in the future that would greatly affect vulnerable

structures. According to our catalogs, the Sumatran Fault produces a very high annual rate of earthquakes, many of which occur in the shallow region under the island of Sumatra (Fig. 1).

1.1 Regional geology and recent earthquakes

The city of Padang, with a population of 856,814 people as of 2008, is the capital of West Sumatra province. The location of the city center is at 100.38°E , 0.95°S . The main part of Padang is situated on an alluvial plain between the Indian Ocean and the mountains. For the most part, the mountainous area is formed of Tertiary sedimentary rocks with outcrops of metamorphic rocks seen in some places. The alluvial plain spreads along the base of the mountains and is roughly 10 km wide in the east-west direction and 20 km wide in the north-south direction.

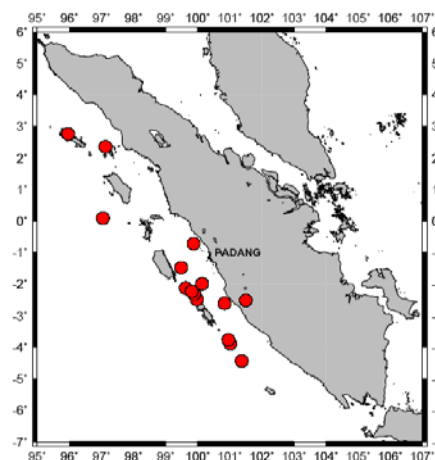


Fig.1 Seismicity of Sumatra Island from 2005 to 2010, Mw>6.5, <100km depth of hypocenter, and Padang City.

The topography of the Padang region (Fig.2) is very similar to the tsunami-damaged area of Miyagi Prefecture in Japan, that was inundated by as much as 4-5 km from the coast after the March 11, 2011 Mw 9.0 Tohoku earthquake off the east coast of Honshu. In Padang, about 600,000 people live in the coastal area (covering about 60 km²).

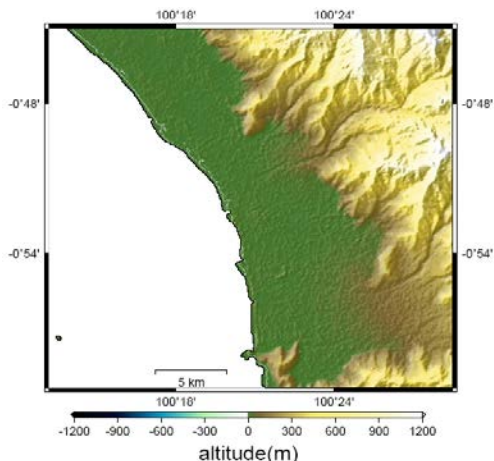


Fig.2 Topography of Padang city

The population density is very high, about 8500 people/km². The city is located on the coast of the Indian Ocean between the Sumatran Fault and the Sunda Trench Fault. Both faults are active with slip rate ranging from 10 to 27 mm/year [2]. According to our catalog, 2995 events with a magnitude greater than 4 occurred in this region from AD 1779 to 2010. The seven giant earthquakes mentioned previously have all been strongly felt here. For example, the source of the 2009 Padang earthquake was located in the ocean slab of the Indo-Australian Plate. It produced extensive shaking and severe damage to houses and buildings in Padang and Padang Pariaman, because its epicenter was about 60 km offshore from Padang Fig. 2. As the Padang earthquake was an intra-slab earthquake at intermediate depth with a comparable magnitude, the event did not generate a tsunami of significance [3]. Due to this earthquake, 1117 people were reported killed, 1214 severely injured, 1688 slightly injured, and 3 were left missing in West Sumatra. The earthquake also destroyed many houses, buildings and infrastructure (heavily damaged houses numbered 114,797, with 67,198 moderately damaged and 67,837 slightly damaged). In Padang, 5458 buildings sustained damage [4]. This event occurred at the end of the working day, just 15 minutes after offices and schools closed; if it had struck earlier, the number of casualties would definitely have been higher as a result of building collapses. Several hours after Padang earthquake, 1st October 2009, Sumatran fault line generated Mw7.1 and 10km depth. Due to this earthquake destroyed many houses and building (heavily

damaged houses numbered 600, with 550 moderately damaged)[5].

There are four accelerometers in Padang. Three were donated by Engineers Without Borders Japan (EWBJ) and installed in 2008, and the other was installed by the Indonesian Government's Bureau of Meteorology, Climatology and Geophysics (BMKG). However, only one ground motion record is available for the Padang earthquake. Due to an electric power cut during the earthquake, only the BMKG device recorded the time history of the earthquake. The observed record shows about 20 s of strong shaking with a peak ground acceleration (PGA) of 0.3 g and a predominant period of 0.5 s (Fig. 2(b)). Response spectra at low period is greater than Indonesia code for rock condition (0.83g) [6]. The location of this station is a mountainous suburb about 12 km in from the coast. The subsurface condition at this station is rocky; the average shear wave velocity for the this rocky is >300m/s² [7].

2. SITE CHARACTERIZATION BY MICROTREMOR OBSERVATION

2.1 Single Observation

A microtremor is a very small ground motion that can be recorded on the ground surface. It can be produced by a variety of excitations (e.g., wind, traffic, breaking sea waves). A full microtremor record can be described by one vertical and two horizontal components. Our analysis was conducted using the recorded microtremor. First, the horizontal and vertical spectrum ratios (HVSr) were computed for all sites (Fig. 3). HVSr (Horizontal-Vertical Spectra Ratio) is consists in estimating the ratio between the Fourier amplitude spectra of the horizontal (H) to vertical (V) components of ambient noise vibrations recorded at one single station.

The peak period of the HVSr is known to correspond to the resonant period of the site. This method postulates the shape of the Fourier spectrum. Equation. (1) shows the method used to calculate HVSr using the observed records.

$$HVSr = \sqrt{\frac{F_{NSi}(\omega)^2 + F_{FWi}(\omega)^2}{F_{UDI}(\omega)^2}} \quad (1)$$

where $F_{NSi}(\omega)$ and $F_{UDI}(\omega)$ denote the Fourier amplitude of the NS, EW and UD components of each interval, respectively, and ω is the frequency. We performed 110 single site surveys that sampled every district of the city of Padang. These observations were carried out in November 2008, September, November, and December 2009 and

January 2010. The locations of observations are plotted in Fig.3. Microtremor was measured using a GPL- 6A3P sensor. The two horizontal (NS and EW) and the vertical (UD) components were recorded simultaneously for 10 minutes with a 100 Hz sampling frequency.

We estimated the distribution of the peak periods of the HVSRs for all sites in Padang using the ordinary kriging technique (Fig.4). From single observations, we obtained a predominant period of 2.0 to 4.0 s in the central business district and less than 1.0 s in the mountainous areas. These results

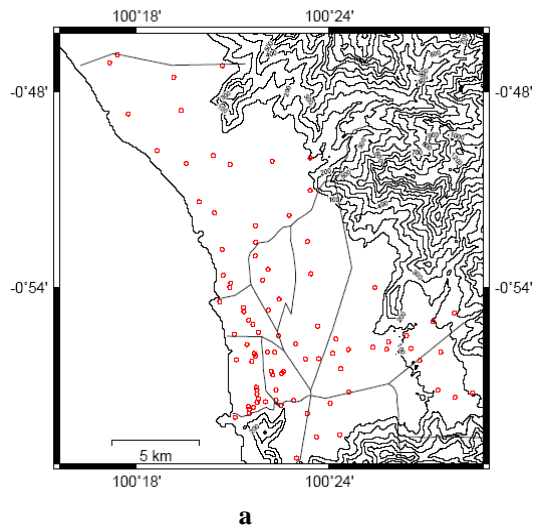


Fig 3. Microtremor single observation sites

indicate an affect related to the thickness of alluvium in the coastal area of Padang city, which decreases in thickness inland.

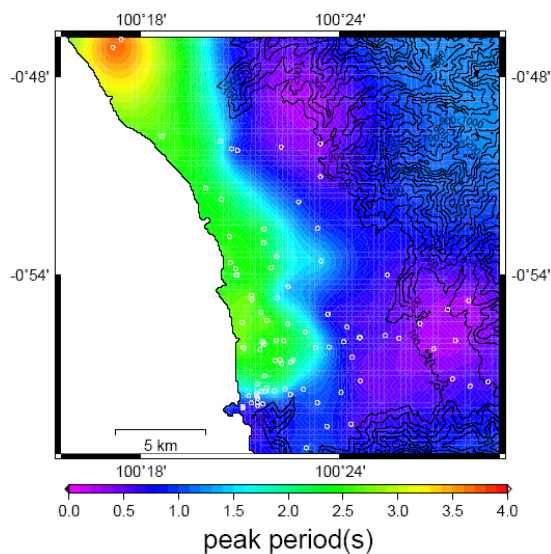


Fig. 4 Distributed HVSR ratio for whole Padang city.

2.2 Microtremor Array Observations

The velocity of surface waves is well known to vary as a function of frequency (or period) due to dispersion. Since dispersion is a function of

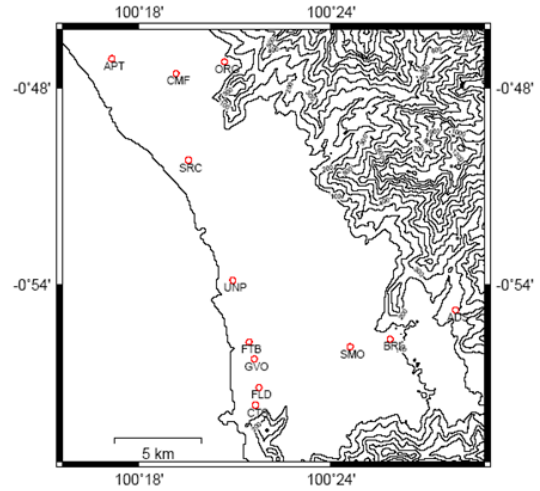


Fig 5. The microtremor array observation sites

subsurface structure, the substructure can be estimated from a Rayleigh wave dispersion curve. We carried out microtremor array investigations using 12 sites at several districts in Padang (Fig.5).

Dispersion curves were calculated using the SPAC method [8] to obtain a velocity structure from the microtremor recordings. An outline of the procedure follows. It is necessary to simultaneously record microtremors with an instrument array of at least three stations. The dispersion of a measured surface wave is a response to the subsurface structure directly below the array, and the estimation of the subsurface structure causing the dispersion is determined by means of inversion of Rayleigh waves. The basic principles of the SPAC method assume that the complex wave motions of microtremors are stochastic processes in time and space. A spatial autocorrelation coefficient for a circular array can then be defined when the waves composing the microtremor (i.e., the surface waves) are dispersive. Hence, the spatial autocorrelation is a function of phase velocity and frequency. Rayleigh wave records were measured for the 12-array observation sites using the SPAC method and inversion analysis was undertaken on the observed dispersion curves to estimate the soil profiles. In the inversion analysis, the Particle Swarm Optimization (PSO) algorithm was adopted to solve the non-linear optimization problem [9]. The basic procedures of PSO are outlined below.

The particle swarm concept originated as a simulation of simplified social system. The original intent was to graphically simulate the choreography of bird of a bird block or fish school. However, it was found that particle swarm model can be used as

an optimizer, PSO simulates the behaviors of bird flocking. Suppose the following scenario: a group of birds are randomly searching food in an area. There is only one piece of food in the area being searched. All the birds do not know where the food is. But they know how far the food is in each iteration. So what's the best strategy to find the food? The effective one is to follow the bird which is nearest to the food. PSO learned from the scenario and used it to solve the optimization problems. In PSO, each single solution is a "bird" in the search space. We call it "particle". All of particles have fitness values which are evaluated by the fitness function to be optimized, and have velocities which direct the flying of the particles. The particles fly through the problem space by following the current optimum particles. PSO is initialized with a group of random particles (solutions) and then searches for optima by updating generations. In every iteration, each particle is updated by following two "best" values. The first one is the best solution (fitness) it has achieved so far. (The fitness value is also stored.) This value is called pbest. Another "best" value that is tracked by the particle swarm optimizer is the best value, obtained so far by any particle in the population. This best value is a global best and called gbest. When a particle takes part of the population as its topological neighbors, the best value is a local best and is called lbest.

We estimate the subsurface structure of the model by solving a nonlinear minimization problem with the fitness function below.

$$v_{id}^{t+1} = \omega v_{id}^t + c_1 r_1 (p_{id}^t - x_{id}^t) + c_2 r_2 (p_{gd}^t - x_{gd}^t) \quad (2)$$

$$x_{id}^{t+1} = x_{id}^t + v_{id}^{t+1} \quad (3)$$

where v_{id}^t is particle velocity of the i^{th} component in dimension d in the interaction, x_{id}^t is the particle position of the i^{th} component in dimension d in interaction, c_1 and c_2 are constant weight factors, p_i is the best position achieved by particle i , p^g is the best position found by the neighbor of particle i , r_1 and r_2 are random factors in the [0,1] interval and ω is the inertia weight. Before performing the inversion analysis, the subsurface structure was assumed to consist of horizontal layers of elastic and homogeneous media above a semi-infinite elastic body. The shear wave velocity and thickness of each layer are the parameters determined by the inversion analysis. The results enable us to determine the condition of shallow subsurface structures [10]. The outline of the SPAC method for the phase velocity calculation of Rayleigh waves follows.

$$F(\omega) = \frac{1}{2\pi} \int_{-\infty}^{\infty} f(t) \cdot \exp(-i\omega t) dt = A_f(\omega) \cdot \exp(-i\phi_f(\omega)) \quad (4)$$

$$G(\omega) = \frac{1}{2\pi} \int_{-\infty}^{\infty} g(t) \cdot \exp(-i\omega t) dt = A_g(\omega) \exp(-i\phi_g(\omega)) \quad (5)$$

$A_f(\omega)$, $A_g(\omega)$ and $\phi_f(\omega)$, are difference between the amplitude of $\phi_g(\omega)$, $F(\omega)$, $G(\omega)$ respectively. Further cross correlation in the frequency region of the two waveforms will be as follows.

$$= F(\omega) \cdot \overline{G(\omega)} = A_f(\omega) \cdot A_g(\omega) \cdot i\Delta\phi(\omega) \quad (6)$$

It shows the phase difference of $\Delta\phi(\omega)$

$$\Delta\phi(\omega) = \frac{\omega r}{c(\omega)} \quad (7)$$

$c(\omega)$ is the phase velocity from the phase difference.

$$CC_{fg} = A_f(\omega) \cdot A_g(\omega) \cdot \exp\left(i \frac{\omega r}{c(\omega)}\right) \quad (8)$$

The complex coherence of two waveforms is defined by the following equation.

$$COH_{fg}(\omega) = \frac{CC_{fg}(\omega)}{A_f(\omega) \cdot A_g(\omega)} = \exp\left(i \frac{\omega r}{c(\omega)}\right) \quad (9)$$

$$Re(COH_{fg}(\omega)) = \cos\left(i \frac{\omega r}{c(\omega)}\right) \quad (10)$$

$$c(\omega, \varphi) = \frac{c(\omega)}{\cos\varphi} \quad (11)$$

$$SPAC(\omega, r) = \frac{1}{2\pi} \int_0^{2\pi} \exp\left(i \frac{\omega r}{c(\omega)} \cos\varphi\right) d\varphi \quad (12)$$

$$Re(SPAC(\omega, r)) = \frac{1}{2\pi} \int_0^{2\pi} \cos\left(i \frac{\omega r}{c(\omega)} \cos\varphi\right) d\varphi \quad (13)$$

$$J\left(\frac{\omega r}{c(\omega)}\right) = \frac{1}{2\pi} \int_0^{2\pi} \exp\left(\frac{\omega r}{c(\omega)} \cos\varphi\right) d\varphi \quad (14)$$

where $J_0(x)$ is the zero-order Bessel function of the first kind of x, and $c(\omega)$ is the phase velocity at frequency ω . The SPAC coefficient $\rho(r, \omega)$ can be obtained in the frequency domain using the Fourier transform of the observed microtremors.

From the SPAC coefficient $\rho(r, \omega)$, the phase velocity is calculated for every frequency from the Bessel function argument of equation. 15 and the velocity model can be invert. The layer thickness and the average S-wave velocity in Figure 6 each

array site. For the average S wave velocity model obtained by averaging the estimated ground is estimated as a weighted layer thickness. Bessel function argument of equation. 15 and the velocity model can be invert. The layer thickness and the average S-wave velocity in Figure 6 each array site. For the average S wave velocity model obtained by averaging the estimated ground structure of the array site was to be calculated by a weighted average using a S-wave velocity structure is estimated as a weighted layer thickness.

$$Re(SPAC(\omega, r)) = J\left(\frac{\omega r}{c(\omega)}\right) \quad (15)$$

From the SPAC coefficient $\rho(r, \omega)$, the phase velocity is calculated for every frequency from the structure of the array site was to be

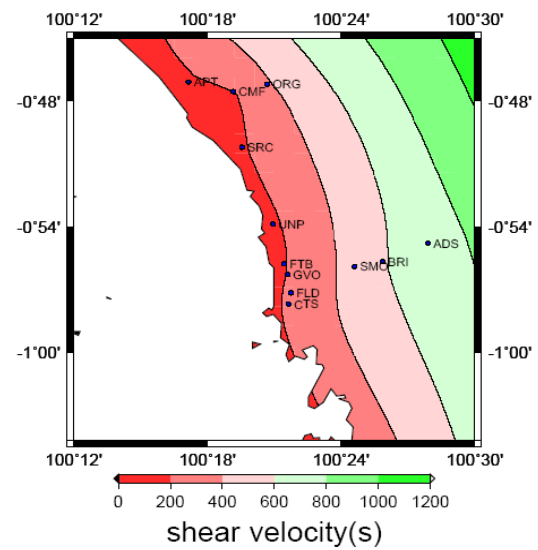


Fig 6. The plotted V_{s30} for whole Padang city

Table 1. Results of microtremor array observations (V_s , average shear wave velocity of the upper 30 m)

Site name	1 st layer		2 nd layer		3 rd layer		4 th layer		Average $V_{s(30)}$
	Thickness (m)	V_s (m/sec)							
ADS	3	163	8	409	~	1891.3	-	-	693
BRI	7	344	13.8	526	38.9	744	~	1219	600
SMO	1.9	135	9.7	468	35.7	508	~	789.4	506
GVO	43.8	198	17.8	308	35.3	356.7	~	515.3	198
FTB	21	158	45	263	35.1	378.8	~	432.4	189
UNP	28.2	163.2	59.3	284	~	469	-	-	171
CTS	5.2	96.8	12.5	184	44.8	296.8	~	471.6	233
FLD	17.7	177	35.6	315	13	410.3	~	479.6	232
ORG	26.1	372.4	12.6	492	~	1266.3	-	-	388
CMF	5.7	163	30.7	197	77.2	293.6	~	423.8	190
SRC	30	190	40.2	257	~	290	-	-	190
APT	20.5	146.7	53.1	234	102	348.7	~	555.3	175

calculated by a weighted average using a S-wave velocity structure

$$\bar{V}_s = \sum V_{si} \cdot \frac{H_i}{H} \quad (16)$$

From the dispersion curve, we can produce an interpretation V_{s30} (average shear wave velocity for the upper 30 m) as show in Table 1, shows the contours of V_{s30} for every 200 m/s increment and soil characteristic every layer. The same procedure applied to get the plotted of V_{s30} for Palu city in Central Sulawesi [11,12]. By using the equation 16, the V_{s30} for whole Padang city is plotted at Fig.6.

3. CONCLUSION

According to microtremor observations, downtown Padang is underlain by soft soil conditions ($V_{s30} < 400$ m/s). Consistent results concerning the soil condition were found based on predominant period observations. In both cases, the coastal area was determined to have a soft soil conditions ($V_{s30} < 400$ m/s), a longer predominant period, and a greater seismic intensity. Padang has a thick alluvial layer in the coastal area (with a predominant period between 2.0 and 4.2 s) that thins toward the mountains (with a predominant period less than 2.0 s). The subsurface geology also

changes slowly from soft soil in the coastal area to rocky conditions in the mountains. The results show clear information on soil condition especially at the downtown, government needs to improve building resistant to earthquake risk by considering propose new local government's regulation on building code.

4. ACKNOWLEDGEMENTS

The author would like to thank to Professor Junji Kiyono from Kyoto University who provided strong support throughout the period. Thanks also go to Professor Yusuke Ono and Professor Noguchi from Tottori University, Japan for their great assistance during the field survey. Thanks to Professor Yanuar Kiram, Dr. Alwen Bentri and Totoh Handayono from University Negeri Padang, Indonesia for their great contributions and ideas during research period. Finally would like to thanks Indonesian government through Universitas Negeri Padang (PNBP foundation) who provided financial support for this research.

5. REFERENCES

- [1] Prawirodirjo, L., Y. Bock, J.F. 2000, One Century of Tectonic Deformation along the Sumatran Fault from Triangulation and Global Positioning System Surveys, *J. of Geophysical research*, 105, 28, 343-28,363.
- [2] Natawidjaja and Wahyu Triyoso 2007. The Sumatran Fault Zone-from Source to Hazard, *J. of Earthquake and Tsunami*, Vol. 1 No. 1, 21-47.
- [3] EERI 2009. The M_w 7.6 Western Sumatra Earthquake of September 30, 2009, Special report.
- [4] BNPB 2009. Total Damage Report and Verification for West Sumatra due to Padang Earthquake, BNPB report, 2009.
- [5] Rusnardi Rahmat Putra, Junji Kiyono, Aiko Furukawa, Assessment of Non Engineering Houses Based on Ddamage Data of the 2009 Padang Earthquake in Padang City, *International Journal of Geomate*, Vol 7, No.2 (SI.No.14) pp.1076-1083,2014
- [6] Rusnardi Rahmat Putra, J. Kiyono, Y. Ono, H Parajuli. 2012, Seismic Hazard Analysis for Indonesia, *Journal of Natural Disaster Science*, Vol. 33, No.3 pp.59-70, June 2012.
- [7] Rusnardi Rahmat Putra, Junji Kiyono, Yusuke Ono, Estimation of Earthquake Ground Motion in Padang City, Indonesia, *International Journal of Geomate*, Vol.1 (S1.No.1), pp.71-77, 2011
- [8] Aki, K. 1957. Space and Time Spectra of Stationary Stochastic Waves, with Special Reference to Microtremor, *Bull. Earth. Res. Inst.*, Vol. 35, No. 3, 415-456.
- [9] Keneddy, J. and Eberhart, R. C. (1995), Particle Swarm Optimization, *Proc. Of IEEE International conference on Neural Networks*, Vol.4,pp.1942-1948.
- [10] Ono, Y., Kiyono, J., Rusnardi, P. R. and Noguchi, T. 2010. Microtremor Observation in Padang City, Indonesia to Estimate Site Amplification of Seismic Ground Motion, *Proc. of International Symposium on a Robust and Resilient Society against Natural Hazards and Environmental Disasters and the third AUN/SEED-Net Regional Conference on Geodisaster Mitigation*, pp.386-391.
- [11] Rusnardi Rahmat Putra, Junji Kiyono, Yusuke Ono, Yasuo Yoshimoto, Syharil, Determined Soil Characteristic of Palu in Indonesia by Using Microtremor Observation, *International Journal of Geomate*, Vol. 10, No.2 (SI. No. 20) 1737-1742, 2016
- [12] Thein, P.S., Pramumijoyo, S., Brotopuspito, K.S., Setianto, A., Rusnardi Rahmat Putra Designed Microtremor Array Based Actual Measurement and Analysis of Strong Ground motion at Palu City, Indonesia, *AIP Conference Proceedings*, 2016.

Copyright © Int. J. of GEOMATE. All rights reserved, including the making of copies unless permission is obtained from the copyright proprietors.
